13 Zhang M, Zamore PD, Carmo-Fonseca M, Lamond AI, Green MR. Cloning and intracellular localization of the U2 small nuclear ribonucleoprotein auxiliary factor small subunit. *Proc Natl Acad Sci USA* 1992; **89**: 8769–8773.
14 Edmond V, Brambilla C, Brambilla E, Gazzeri S, Eymin B. SRSF2 is required for sodium butyrate-mediated p21(WAF1) induction and premature senescence in human lung carcinoma cell lines. *Cell Cycle* 2011; **10**: 1968–1977.
15 Emanuel PD. Juvenile myelomonocytic leukemia and chronic myelomonocytic leukemia. *Leukemia* 2008; **22**: 1335–1342.

Supplementary Information accompanies the paper on the Leukemia website (http://www.nature.com/leu)

Sequencing histone-modifying enzymes identifies UTX mutations in acute lymphoblastic leukemia

Leukemia (2012) **26,** 1881–1883; doi:10.1038/leu.2012.56

Mutations affecting epigenetic regulators have long been known to have a crucial role in cancer and, in particular, hematological malignancies.[1,2] One of the earliest epigenetic factors described altered in leukemia was the mixed lineage leukemia (*MLL*) protein which is found translocated in 10% of adult acute myeloid leukemia (AML), 30% of secondary AML and >75% of infants with both AML and acute lymphocytic leukemia (ALL). *MLL* is a SET domain-containing protein, which is recruited to many promoters and mediates histone 3 lysine 4 (H3K4) methyltransferase activity, thought to promote gene expression.[3]

In addition to *MLL* fusions, recently, somatic mutations of *UTX* (also known as *KDM6A*), encoding an H3K27 demethylase, were described in multiple hematological malignancies, including multiple myeloma and many types of leukemia cell lines.[4,5] H3K27 methylation is generally thought to cause gene repression. Complimentary to *UTX,* mutations of *EZH2*, a H3K27 methyltransferase, have been reported in both lymphoid and myeloid tumors (Figure 1).[6,7] These mutations lead to altered EZH2 activity and influence H3K27 in tumor cells. Mutations in EZH2, EED and SUZ12, which all cooperate in Polycomb repressive complex 2 have been recently described in early T-cell precursor ALL.[8] Similarly, point mutations affecting the functional jumonji C (jmjC) domain of UTX inactivates its H3K27 demethylase activity. In addition, UTX associates with MLL2 in a multiprotein complex, which promotes H3K4 methylation, and recently *MLL2* has also been found mutated in cancer, further pointing to a common and complex epigenetic deregulation in cancer.[9] In line with the growing evidence for epigenetic regulators as important in tumorigenesis, additional mutations affecting epigenetic regulators such as SETD2, a H3K36 methyltransferase, KDM3B, a H3K9 demethylase, and KDM5C, a H3K4 demethylase, have been reported and are associated with distinct gene expression patterns (Figure 1).[4]

Though the clinical significance of these findings remains to be explored, it is evident that epigenetic deregulation is having an important role in both lymphoid and myeloid leukemogenesis. Furthermore, with novel drugs at hand, such as histone deacetylase inhibitors or demethylating agents that can target and reverse epigenetic alterations, understanding the underlying molecular aberrations is of growing interest.[10] We therefore undertook an effort to examine the prevalence of somatic mutations in genes encoding histone-modifying proteins, in particular, *KDM3B*, *KDM5C*, *UTX*, *MLL2*, *EZH2* and *SETD2*, which previously were reported mutated in cancer.[4,5]

For an initial screen, we analyzed banked diagnostic primary leukemia samples from 44 childhood B-cell ALL and 50 adult AML patients, and, where available, used bone marrow samples obtained in complete remission to validate the somatic nature of the mutations. Samples had been collected with patient/parental informed consent from patients enrolled on Dana–Farber Cancer Institute protocols for childhood ALL (DFCI 00-001 (NCT00165178), DFCI 05-001 (NCT00400946)) or AML treatment protocols of the German-Austrian AML Study Group (AMLSG) for younger adults (AMLSG-HD98A (NCT00146120), AMLSG 07-04 (NCT00151242)), and the study was approved by the IRB of the participating centers.

Using conventional Sanger sequencing of primary leukemia sample-derived genomic DNA, we first screened all coding exons in which mutations have been reported previously.[4,5] Initially, we analyzed a total of 36 of 174 exons (*KDM3B* (2/24), *KDM5C* (9/26), *UTX* (7/29), *MLL2* (8/54), *EZH2* (1/20) and *SETD2* (9/21)) and found 7 non-synonymous tumor-specific aberrations. In AML, we found one *EZH2* mutation (p.G648E) in a t(8;21)-positive, and two *MLL2* missense mutations (p.R5153Q and p.Y5216S; Table 1) and one

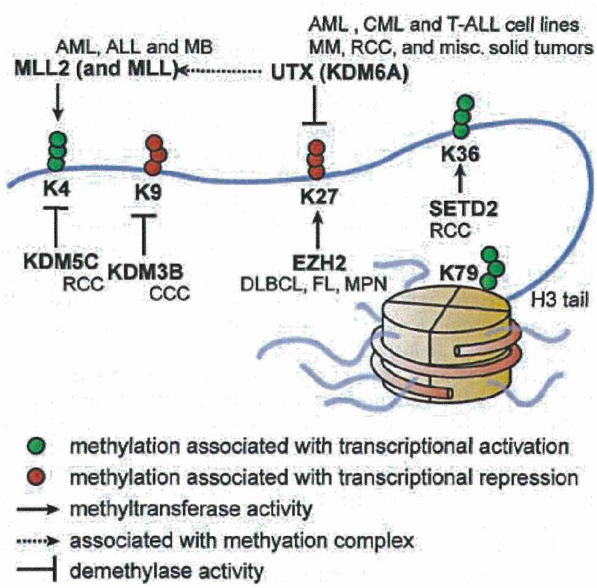

Figure 1. Histone 3 methylation and selected histone demethylases and methyltransferases. Cancers are shown in italics next to the mutated protein they are associated with. MM, multiple myeloma; FL, follicular lymphoma; DLBCL, diffuse large B-cell lymphoma; RCC, renal cell carcinoma; CCC clear cell carcinoma; MPN, myeloproliferative neoplasm; MB, medulloblastoma.

Accepted article preview online 1 March 2012; advance online publication, 3 April 2012

Oncogene (2012) **31,** 4667 - 4676

www.nature.com/onc

ORIGINAL ARTICLE

Aberrant activation of ALK kinase by a novel truncated form ALK protein in neuroblastoma

J Okubo[1], J Takita[1,2], Y Chen[1], K Oki[1], R Nishimura[1], M Kato[1], M Sanada[3], M Hiwatari[1], Y Hayashi[4], T Igarashi[1] and S Ogawa[3]

Anaplastic lymphoma kinase (ALK) was originally identified from a rare subtype of non-Hodgkin's lymphomas carrying t(2;5)(p23;q35) translocation, where ALK was constitutively activated as a result of a fusion with nucleophosmin (NPM). Aberrant ALK fusion proteins were also generated in inflammatory fibrosarcoma and a subset of non-small-cell lung cancers, and these proteins are implicated in their pathogenesis. Recently, ALK has been demonstrated to be constitutively activated by gene mutations and/or amplifications in sporadic as well as familial cases of neuroblastoma. Here we describe another mechanism of aberrant ALK activation observed in a neuroblastoma-derived cell line (NB-1), in which a short-form ALK protein (ALK^{del2-3}) having a truncated extracellular domain is overexpressed because of amplification of an abnormal *ALK* gene that lacks exons 2 and 3. ALK^{del2-3} was autophosphorylated in NB-1 cells as well as in ALK^{del2-3}-transduced cells and exhibited enhanced *in vitro* kinase activity compared with the wild-type kinase. ALK^{del2-3}-transduced NIH3T3 cells exhibited increased colony-forming capacity in soft agar and tumorigenicity in nude mice. RNAi-mediated ALK knockdown resulted in the growth suppression of ALK^{del2-3}-expressing cells, arguing for the oncogenic role of this mutant. Our findings provide a novel insight into the mechanism of deregulation of the ALK kinase and its roles in neuroblastoma pathogenesis.

Oncogene (2012) **31,** 4667–4676; doi:10.1038/onc.2011.616; published online 16 January 2012

Keywords: neuroblastoma; *ALK*; truncated form ALK; amplification

INTRODUCTION

Anaplastic lymphoma kinase (ALK) (OMIM: 105590) is an orphan receptor tyrosine kinase (RTK) that was initially characterized as a fusion partner of the nucleophosmin (NPM)-ALK chimeric protein associated with the t(2;5)(p23;q35) translocation in anaplastic large-cell lymphoma.[1,2] Subsequent studies have revealed that various ALK-containing fusion proteins with different fusion partners are generated in various solid tumors, such as inflammatory myofibroblastic tumors, non-small-cell lung cancer and squamous cell carcinoma of the esophagus.[3-6] Furthermore, recent genome-wide studies have revealed that *ALK* is activated by gene amplification and nucleotide mutations and is involved in the pathogenesis of both familial and sporadic neuroblastoma.[7-10]

Neuroblastoma is an intractable, solid tumor of childhood arising from the neural crest and can arise anywhere along the sympathetic nervous system.[11] The overall 5-year survival rate for neuroblastoma is $\leqslant$40%, despite current intensive multimodality treatments.[12-14] Considering that *ALK* mutations preferentially involve advanced neuroblastoma with a poor outcome, the more relevant implication of these findings is that ALK inhibitors may improve the clinical outcome of children suffering from intractable neuroblastoma.

In this study, we demonstrated another mechanism of aberrant ALK activation in neuroblastoma, in which an abnormal *ALK* gene with a deletion of exons 2 and 3 was amplified in a neuroblastoma-derived cell line (NB-1), leading to high-level expression of an ALK protein variant with a truncated extracellular domain (ALK^{del2-3}). Furthermore, we demonstrated that ALK^{del2-3} had constitutive kinase activity and showed a transforming capacity in NIH3T3 cells. Moreover, ALK inhibition experiments using small interfering RNA (siRNA)-mediated gene knockdown and the low-molecular-weight compound, TAE684, also supported the oncogenic role of ALK^{del2-3}. Our results will help elucidate the mechanism of aberrant activation of ALK kinase and the role of activated ALK in the pathogenesis of neuroblastoma.

RESULTS

Detection of a short-form ALK protein in NB-1 cells

To examine the status of ALK in neuroblastoma, western blotting analysis was performed with a panel of 24 neuroblastoma-derived cell lines (Table 1). Among the 24 samples examined, the NB-1 cell line showed high-level expression of an ALK protein having a low molecular weight of 208 kDa compared with the molecular weight of 220 kDa for the wild-type protein (Figure 1a). Subsequent sequencing and reverse transcription–polymerase chain reaction (RT–PCR) analysis of *ALK* messages from NB-1 cells revealed the presence of an aberrant *ALK* transcript with a 285-bp in-frame deletion in the 5′ region corresponding to exons 2 and 3 (Figures 1b and c), which should result in the production of an abnormal ALK protein with a truncated N-terminal extracellular domain. Using a primer set for exons 2 and 3, a 166-bp product was also detected in NB-1 cells, indicating the presence of the wild-type *ALK* allele in NB-1 cells (Figures 1b and c). The deletion spanned 224–318 amino acids (aa), including the N-terminal end of the first meprin A5 protein and receptor protein tyrosine phosphatase mu (MAM) domain (aa 264–427) (Figure 1d).[15,16] We analyzed full-length *ALK* cDNAs isolated from 71 primary neuroblastoma samples for possible nucleotide deletions using RT–PCR (Table 2), but no deletions were detected.

[1]Department of Pediatrics, Graduate School of Medicine, University of Tokyo, Tokyo, Japan; [2]Department of Cell Therapy and Transplantation Medicine, Graduate School of Medicine, University of Tokyo, Tokyo, Japan; [3]Cancer Genomics Project, Graduate School of Medicine, University of Tokyo, Tokyo, Japan and [4]Gunma Children's Medical Center, Maebashi, Japan. Correspondence: Dr J Takita, Cell Therapy and Transplantation Medicine, Graduate School of Medicine, University of Tokyo, 7-3-1, Hongo, Bunkyo-ku, Tokyo 113-8655, Japan. E-mail: jtakita-tky@umin.ac.jp
Received 22 May 2011; revised and accepted 29 November 2011; published online 16 January 2012

Table 1. Neuroblastoma cell lines used in this study

Cell line	*MYCN amplification*	*ALK status*
CHP-134	–	WT
GOTO	+	WT
LAN-1	+	F1174L
LAN-2	+	WT
LAN-5	+	R1275Q
NB-1	–	Amplification
NB-16	+	WT
NB-19	+	WT
NB-69	–	WT
NH-12	+	WT
SCMC-N2	+	F1174L
SCMC-N4	+	WT
SCMC-N5	+	K1062M
SJNB-1	–	WT
SJNB-2	+	R1275Q
SJNB-3	–	WT
SJNB-4	+	F1174L
SJNB-5	+	WT
SJNB-6	+	WT
SJNB-7	+	WT
SJNB-8	+	WT
SK-N-SH	–	F1174L
TGW	+	R1275Q
UTP-N-1	+	WT

Abbreviations: ALK, anaplastic lymphoma kinase; WT, wild type.

Structural abnormality of the *ALK* gene in NB-1 cells

As reported previously,[7] our single-nucleotide polymorphism array-based copy number analysis of NB-1 cells disclosed high-level gene amplification of the *ALK*-containing 2p24 segment. This should explain the high *ALK* expression observed in this cell line (Figures 1a and b). In particular, the genomic copy numbers within the 2p23 amplicon exhibited a transient decrease at three consecutive single-nucleotide polymorphisms (Chr2: 29 911 541–29 912 210), which corresponded to *ALK* intron 3, raising the possibility that a gene deletion involving exons 2 and 3 was responsible for the aberrant *ALK* transcript (Figure 2a). To confirm this, we performed Southern blot analysis of NB-1 genomic DNA using fragments exons 1–4 as probes (Figure 2b). As shown in Figures 2c–e, Southern blot analysis confirmed *ALK* gene amplification in NB-1 cells, as these blots showed high-intensity signals for each of the four *ALK*-specific probes in NB-1 cells compared with those in the controls. However, a significant difference was observed in the signal intensity between the fragments containing exons 1/4 and exons 2/3 in the NB-1 lanes, in which exons 1 and 4 showed 3.9- and 3.8-fold higher signals than exons 2 and 3, respectively. This result was confirmed by quantitative genomic PCR analysis using seven primer sets located within *ALK* exons 1–4 (Figure 2f). Taken together, these results indicate that the 2p23 amplicons were heterogeneous with regard to the species of *ALK* it contained, among which the predominant *ALK* allele had a deletion at exons 2 and 3, and these amplicons were responsible for the generation of $ALK^{del2\text{-}3}$.

Oncogenic potential of an aberrant short-form ALK protein

We next evaluated the oncogenic role of the truncated form of ALK found in NB-1 cells in terms of its kinase activity. As shown in Figure 3a, $ALK^{del2\text{-}3}$ was strongly phosphorylated in NB-1 cells, whereas the wild-type ALK expressed in NH-12 cells was unphosphorylated. Similar to the constitutive active F1174L ALK mutant when expressed in NIH3T3 cells, $ALK^{del2\text{-}3}$ had enhanced ALK phosphorylation compared with wild-type ALK (Figure 3b). Moreover, after anti-FLAG immunoprecipitation of FLAG-tagged ALK constructs, $ALK^{del2\text{-}3}$ and F1174L ALK mutants were strongly phosphorylated according to western blot analysis using a PY20 blot (Figure 3c). In addition, they exhibited enhanced kinase activity in an *in vitro* kinase assay using the YFF peptide as a substrate (Figure 3d). To confirm kinase activity of the $ALK^{del2\text{-}3}$ mutant, we further examined *in vitro* kinase activities of wild-type and mutant ALK-expressing NIH3T3 cells using a universal substrate. The immunoprecipitated FLAG-tagged $ALK^{del2\text{-}3}$ mutant showed significantly increased kinase activity (Supplementary Figure S1).

In an analysis of activated downstream signaling, significantly enhanced STAT3 phosphorylation was observed in $ALK^{del2\text{-}3}$ and F1174L mutants, whereas a significant increase in AKT phosphorylation was not detected in any samples (Figure 3e and Supplementary Figure S2). Extracellular regulated kinase (ERK) was probably phosphorylated in the F1174L mutant and wild-type ALK, but not in $ALK^{del2\text{-}3}$ (Figure 3e). The results of three independent experiments were quantified by densitometric scanning (Supplementary Figure S2).

We investigated the oncogenic potential of the $ALK^{del2\text{-}3}$ mutant in NIH3T3 cells, in terms of colony formation in soft agar and tumor generation in nude mice. As shown in Figures 4a and b, NIH3T3 cells that were stably transduced with $ALK^{del2\text{-}3}$ and ALK^{F1174L} produced a significantly higher numbers of colonies in soft agar than mock or wild-type *ALK*-transduced cells (Figures 4a and b). When inoculated into nude mice, the $ALK^{del2\text{-}3}$-transduced NIH3T3 cells invariably developed into subcutaneous tumors (5/5), whereas the mock and wild-type *ALK*-transfected cells did not develop into tumors (0/5) (Figure 4c).

$ALK^{del2\text{-}3}$ was retained in the endoplasmic reticulum

Among ALK signaling pathway molecules, STAT3 was only strongly phosphorylated by $ALK^{del2\text{-}3}$, suggesting that the $ALK^{del2\text{-}3}$ mutant was exclusively involved in the STAT3 pathway. It has been previously reported that intracellular fms-like tyrosine kinase-internal tandem duplication activation induces an aberrant downstream signaling outcome.[17] To determine whether $ALK^{del2\text{-}3}$ expresses at the cell surface and mediates signals from endoplasmic reticulum (ER), we analyzed localization and deglycosidation of $ALK^{del2\text{-}3}$ in NB-1 cells and wild-type ALK in NH-12 cells. Immunofluorescence staining revealed that ALK in NB-1 cells was almost colocalized with PDI, whereas ALK in NH-12 cells was largely located at the plasma membrane (Figure 5a). As shown in Supplementary Figure S4, colocalization of ALK and PDI was quantified using the Pearson's correlation coefficient. Moreover, to determine whether $ALK^{del2\text{-}3}$ was subjected to maturation of its oligosaccharides, we examined the endoglycosidase H sensitivity of ALK expressed in NB-1 and NH-12 cells. As shown in Figure 5b, $ALK^{del2\text{-}3}$ in NB-1 cells revealed the high sensitivity of endoglycosidase H compared with the wild-type ALK in NH-12 cells, suggesting that intercellular localization of $ALK^{del2\text{-}3}$ was associated with a defect in N-linked glycosylation.[18] These results indicate that $ALK^{del2\text{-}3}$ is mainly located at ER and aberrantly activates the STAT3 pathway from there.

Effect of ALK inhibition on cell growth in NB-1 cells

Finally, we examined the effect of ALK inhibition on NB-1 cell proliferation using the small-molecule ALK inhibitor TAE684 and siRNA-mediated ALK knockdown. NB-1 cell growth was effectively inhibited by TAE684 with a half maximal inhibitory concentration (IC_{50}) of 13 nM, which was similar to the IC_{50} for SK-N-SH (49 nM; an *ALK*-mutated TAE684-sensitive neuroblastoma cell line), but substantially lower than the IC_{50} for TGW cells with the ALK^{R1275Q} mutant (310 nM), the glioblastoma-derived cell line H4 with wild-type ALK (190 nM) and NIH3T3 cells with no ALK expression (380 nM) (Figure 6a). Similarly, siRNA-mediated knockdown of $ALK^{del2\text{-}3}$ in NB-1 cells resulted in significant suppression of cell proliferation compared with controls transfected with nonspecific

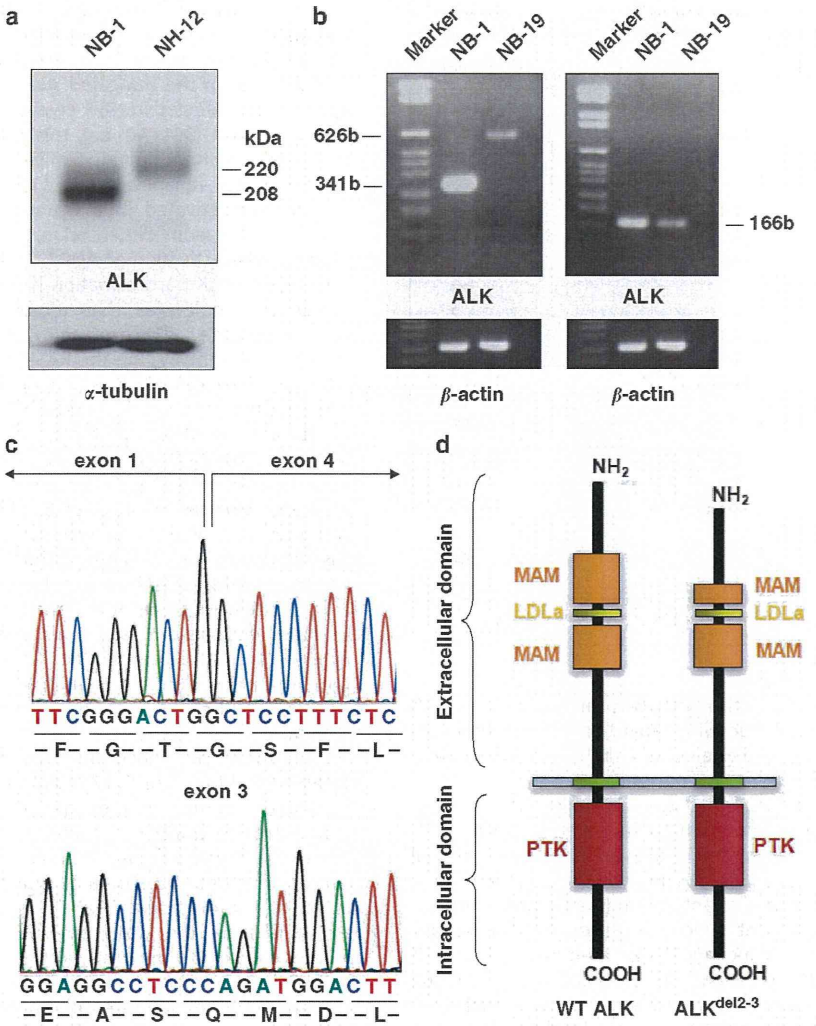

Figure 1. Detection of an aberrant truncated form of ALK in NB-1 cells. (**a**) Western blot analysis of ALK in neuroblastoma-derived cell lines. NB-1 cells strongly expressed the truncated form with a molecular mass of 208 kDa. In contrast, wild-type ALK-expressing neuroblastoma-derived cell lines (NH-12) revealed an ALK protein with a molecular mass of 220 kDa. α-Tubulin staining as loading control. (**b**) RT-PCR analysis of *ALK* exons 1–5 and exons 2 and 3 in the neuroblastoma cell lines. A short PCR product with 314 bp was detected in NB-1 cells, whereas much longer PCR products with 627 bp were detected in NB-19 cells with wild-type *ALK*. Wild-type *ALK* was detected in both NB-1 and NB-19 cells using *ALK* exon 2 and 3 primers. (**c**) Subsequent sequence analysis of *ALK* cDNA from NB-1. In-frame deletion in exons 2 and 3 was confirmed by direct sequencing. Sequencing of the PCR product detected by RT-PCR for *ALK* exons 2 and 3 confirmed the presence of wild-type *ALK* in NB-1 cells. Lower panel represents DNA sequencing for *ALK* exon 3 in NB-1 cells. (**d**) Schematic representation of the truncated form of aberrant ALK. The extracellular domain of ALK comprises two MAM domains (aa 264–427 and 480–626), one low-density lipoprotein class A (LDLa) motif (aa 453–471) and a glycine-rich region (aa 816–940) (Palmer *et al.*[30]). Because exons 2 and 3 of *ALK* implicate 224–318 aa, the in-frame deleted mutant led to a translational truncated form of the first MAM domain. PTK, protein tyrosine kinase.

siRNA, but the suppression apparently decreased in wild-type ALK-expressing NH-12 cells (Figures 6b and c). As shown in Supplementary Figure S3, significant inhibition was observed in NB-1 cells with ALK knockdown compared with that in the negative control ($P<0.05$, Mann–Whitney *U*-test).

DISCUSSION

Deregulated activation of ALK has been implicated in various human cancers through either generation of fusion proteins, overexpression or single amino-acid changes. In this study, we described a novel mechanism of oncogenic activation of *ALK* that operated in a neuroblastoma-derived cell line, NB-1. In NB-1 cells, an aberrant form of *ALK* that lacks exons 2 and 3 was amplified, leading to high-level expression of an N-terminal-truncated kinase, ALK^{del2-3}, and our functional studies confirmed the oncogenic role of ALK^{del2-3}. First, ALK^{del2-3} underwent autophosphorylation in NB-1 and NIH3T3 cells and demonstrated enhanced kinase activity, promoting downstream signaling pathways such as the STAT3 pathway. Second, ALK^{del2-3} promoted colony formation in soft agar and tumorigenicity when transduced into NIH3T3 cells in nude mice. Finally, inhibition of cell growth was observed when we treated NB-1 cells with TAE684, an ALK-specific kinase inhibitor, and siRNA-mediated gene knockdown. Unfortunately, screening of 71 primary neuroblastoma specimens and 23 neuroblastoma-derived cell lines did not identify a similar mechanism of ALK oncogenic activation in neuroblastoma; therefore, it is not a common mechanism for ALK activation in

Table 2. Neuroblastoma fresh tumor samples used in this study

Clinicopathological findings	*Samples*
Age (years)	
>1	41
<1	30
Stage	
1	16
2	11
3	12
4	29
4S	2
ND	1
MYCN status	
Amplification (+)	11
(−)	58
ND	2
ALK status	
Amplification	1
Mutation	6
Wild type	64
Total	71

Abbreviations: ALK, anaplastic lymphoma kinase; ND, not determined.

neuroblastoma. Nevertheless, the discovery of this unique ALK form will add to our knowledge with regard to the pathogenesis of neuroblastoma and will help to elucidate the mechanism of ALK activation.

Abnormal activation of RTK through a deletion in its extracellular domain has been documented in several cancers.[19–21] A common example of abnormal RTK activation is the epidermal growth factor receptor class III variant, which is present in a substantial proportion of malignant gliomas and other human cancers, but completely absent in normal tissues.[22,23] This variant results from a transcript having an 801-bp in-frame deletion of EGFR that corresponds to exons 2–7, which leads to the generation of a protein with a truncated extracellular domain.[21,24] Several molecular mechanisms have been implicated in the oncogenic pathway with epidermal growth factor receptor class III variant downstream signaling.[21,24] For example, in addition to ligand-independent self-dimerization, epidermal growth factor receptor class III variant has been shown to constitutively interact with adaptor proteins SHC and GRB2, which are involved in the recruitment of the RAS pathway.[25] The recepteur d'origine nantais (RON) RTK variant with a deletion in the first immunoglobulin-plexin transcription domain (RONΔ160) has also been considered as a constitutively activated kinase in several human cancers.[20,26] RON belongs to the MET proto-oncogene family, which plays a critical role in epithelial cell homeostasis and tumorigenic development.[27] RONΔ160 is derived from a *RON* mRNA transcript by alternative splicing that eliminates 109 aa residues from the extracellular domain of RON β-chain and is expressed in >50% of primary colon cancers and 90% of brain tumors, but not in any normal tissues.[26,28] The deleted 109 aa residues are encoded by exons 5/6, which constitute the first immunoglobulin-plexin transcription domain in the RON β-chain.[26,28] The mechanism for the oncogenic activation of RONΔ160 is believed to be one in which the deletion in the extracellular domain causes conformational changes in the kinase and leads to spontaneous dimerization, which in turn causes constitutive receptor phosphorylation and increased intracellular signaling activation.[26,28,29]

The $ALK^{del2\text{-}3}$ variant consists of a 282-bp in-frame deletion of *ALK* that corresponds to 224–318 aa in the first MAM domain (Figure 1d). ALK is the sole RTK that contains MAM domains in its extracellular region.[30] Although MAM domains are thought to participate in cell–cell interactions, their significance in ALK function remains unclear.[15,16] Thus, the functional significance of MAM deletion in the truncated ALK is still elusive. As the deleted region of *ALK* detected in NB-1 cells is in close proximity to a ligand-binding domain (391–401 aa), this deletion may structurally alter the ligand-binding domain. Similar to epidermal growth factor receptor class III variant and RONΔ160, the $ALK^{del2\text{-}3}$ variant may be constitutively activated in a ligand-independent manner and/or through spontaneous dimerization, although the exact mechanism of constitutive activation of $ALK^{del2\text{-}3}$ is yet to be elucidated.

Oncogenic ALK transformation is mediated by interactions with downstream molecules that trigger a substantial intercellular signaling cascade.[31] The most relevant and best-characterized ALK downstream pathways are the RAS-ERK, JAK3-STAT3 and PI3K-AKT pathways.[31] Among ALK signaling molecules, STAT3 is only strongly phosphorylated by $ALK^{del2\text{-}3}$, suggesting that besides F1174L or K1062M ALK mutants,[7] $ALK^{del2\text{-}3}$ would be exclusively involved in the STAT3 pathway. Recently, it has been reported that the oncogenic mutant of fms-like tyrosine kinase-internal tandem duplication aberrantly activates STAT5 when localized at ER, but fails to activate MAPK and AKT signaling.[17] Thus, this raises the possibility that involvement of the STAT3 pathway in $ALK^{del2\text{-}3}$-expressing cells resembles the fms-like tyrosine kinase-internal tandem duplication mutant.[17] Immunofluorescence staining and the endoglycosidase H sensitivity assay revealed that $ALK^{del2\text{-}3}$ is mainly located at ER and aberrantly activates the STAT3 pathway from ER. Taken together, our results suggest that intracellular activation of $ALK^{del2\text{-}3}$ switches downstream signaling to the ALK pathway.[18]

Furthermore, ERK phosphorylation was similarly elevated in cells expressing wild-type or F1174L ALK. This may have been because of enhanced expression of exogenous wild-type *ALK* by retrovirus-mediated gene transfer. Schulte *et al.*[32] reported that the high level of wild-type ALK and mutant ALK expression has similar effects on the neuroblastoma biological phenotype, which may be related to tumor growth. Taken together, the results from our study and from the study by Schulte *et al.*[32] suggest that in addition to the ALK mutants, elevated wild-type ALK expression also mediates similar molecular functions that contribute to the malignant phenotype in neuroblastoma.

In summary, we found that an N-terminal-truncated ALK protein observed in a neuroblastoma-derived cell line (NB-1) is a novel oncogenic isoform of ALK. This study provides a better understanding of the molecular mechanism of pathogenesis of neuroblastoma as well as oncogenic roles of ALK pathway.

MATERIALS AND METHODS

Specimens

In all, 24 neuroblastoma cell lines were used in this study (Table 1). The SCMC-N series was established in our laboratory.[33] The SJNB series and UTP-N-1 cells were provided by Dr AT Look and Dr A Inoue, respectively. Other cell lines were obtained from the Japanese Cancer Resource Cell Bank (http://cellbank.nibio.go.jp/wwwjcrbj.htm). All cells were maintained in RPMI 1640 medium (Gibco, Grand Island, NY, USA) supplemented with 10% fetal bovine serum in a humidified atmosphere containing 5% CO_2 at 37 °C. Primary neuroblastoma specimens were obtained through surgery or biopsy from patients who were diagnosed with neuroblastoma and who were admitted to Tokyo University Hospital, Saitama Children's Medical Center or various other hospitals between November 1993 and October 2006. The patients were staged according to the International Neuroblastoma Staging System,[34] and the clinicopathological findings are listed in Table 2.

ALK expression analyses

Total cellular proteins were resolved on a 5–10% gradient sodium dodecyl sulfate-polyacrylamide gel and electrophoretically transferred onto

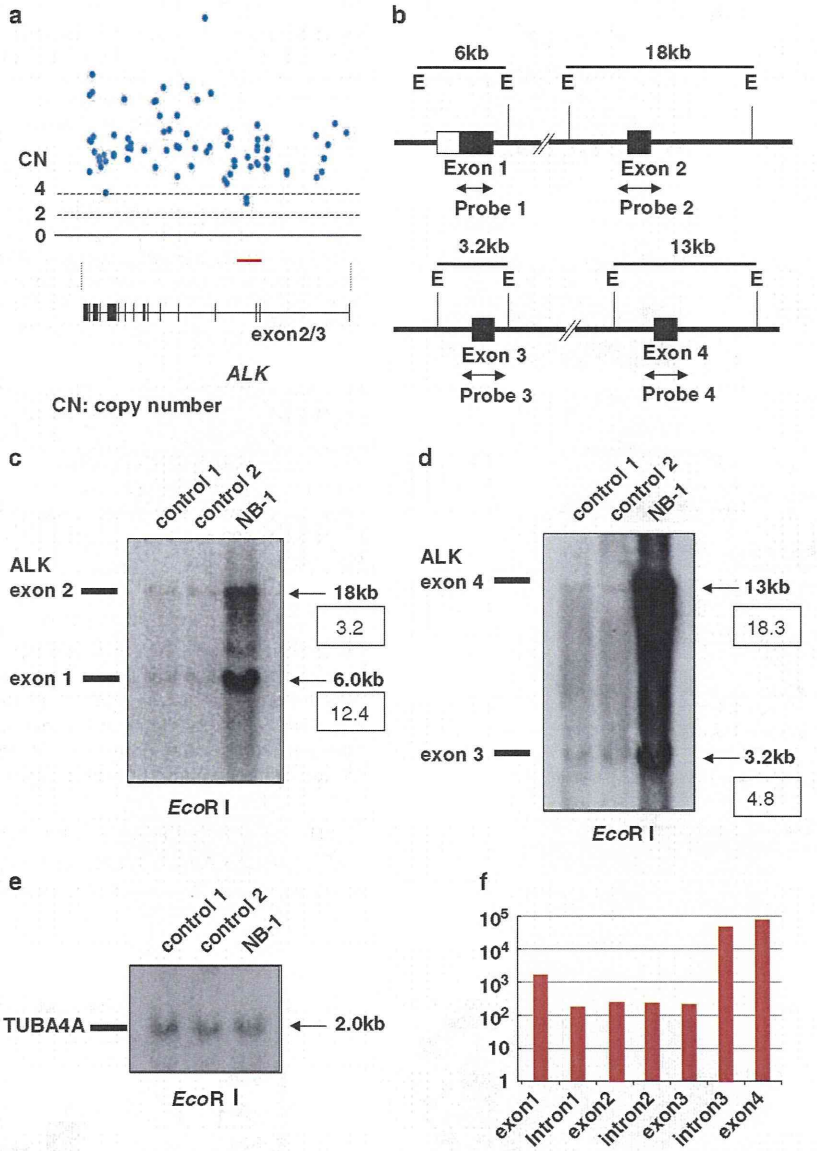

Figure 2. Genetic characteristics of the N-terminal-truncated form of ALK. (**a**) High-grade amplification of the *ALK* locus detected in NB-1 cells by single-nucleotide polymorphism array analysis (Affymetrix GeneChip 250k *Nsp*I). Among the single-nucleotide polymorphism probes located within the *ALK* amplicon, three consecutive single-nucleotide polymorphism probes (Chr2: 29 911 541 and 29 912 210) located within *ALK* intron 3 showed relatively low signal intensities. The red line indicates the focal deletion within *ALK* intron 3. (**b**) Physical maps of *ALK* exons 1–4. The restriction sites and probe maps for *ALK* exons 1–4 are indicated. E: *Eco*R1. Arrows indicate probe positions. (**c**, **d**) Southern blot analysis using *ALK* exon 1–4 probes (**c**: exons 1 and 2; **d**: exons 3 and 4). Normal peripheral blood DNA was used as a germline control. Densitometric analysis was performed using the ImageQuant 400 and ImageQuant TL software version 7. (**e**) The TUBA4A probe was used as a loading control. (**f**) Quantitative genomic PCR analysis of *ALK* using seven primer sets located within *ALK* exons 1–4. The signal intensities of *ALK* introns 1 and 2 and exons 2 and 3 were lower compared with those of *ALK* exons 1 and 4 in NB-1 cells.

polyvinylidene difluoride membranes. After blocking with 5% milk in Tris-buffered saline containing 0.1% Tween (10 mM Tris-HCl (pH 7.4), 150 mM NaCl and 0.1% Tween-20), membranes were incubated for 1 h with primary antibody in TBS-T, washed and incubated for 12 h with primary antibody in 3% bovine serum albumin. The membranes were then washed again and incubated with anti-rabbit immunoglobulin G at room temperature for 1 h. Subsequently, they were extensively washed, and the proteins were visualized by enhanced chemiluminescence (Millipore, Bedford, MA, USA). Total RNA was extracted from the 24 cell lines and 71 frozen stocked tumors using Isogen reagent (Nippon Gene, Osaka, Japan) according to the manufacturer's instructions; the total RNA was analyzed by RT-PCR to synthesize cDNA using the SuperScript Preamplification System for first-strand cDNA synthesis (Life Technologies Inc., Rockville, MD, USA). RT-PCR analysis for *ALK* expression was performed as described previously,[7] using the primer sets listed in Table 3. cDNA concentration was equalized using *β-actin* expression as a control.

Southern blot analysis

High-molecular-weight DNA was prepared from cells according to standard procedures using the QIAamp DNA Mini kit (Qiagen, Valencia, CA, USA) and a modification of the protocol provided by the manufacturer.

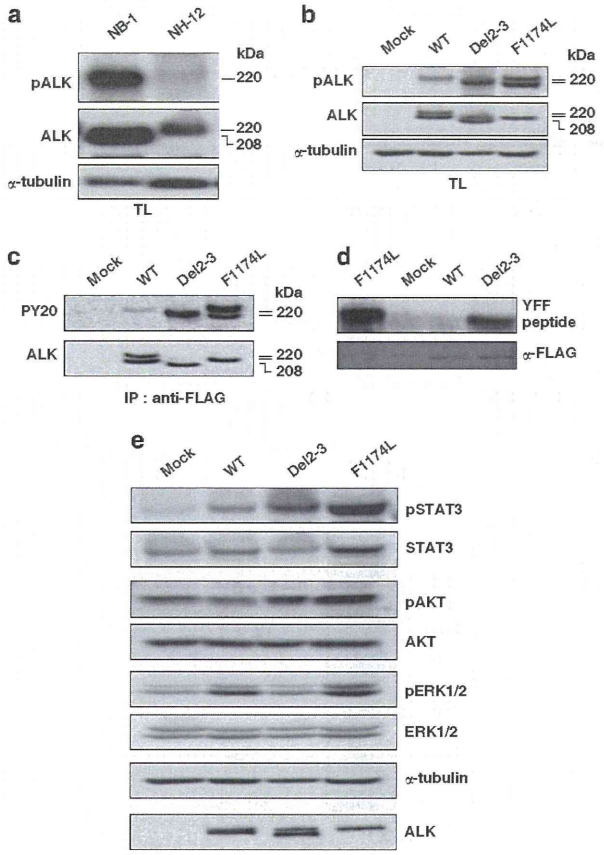

Figure 3. Kinase activities of ALK mutants and their downstream status. (**a**) Western blot analysis of ALK and phosphorylated ALK in NB-1 and NH-12 cells. NB-1 cells strongly expressed the truncated form of ALK and phosphorylated ALK compared with that in NH-12 cells. TL: Total cell lysates. (**b**) Western blot analysis of NIH3T3 cells stably expressing ALK mutants (ALK^{del2-3} and ALK^{F1174L}) and wild-type ALK. (**c**) Stably expressed ALK mutants and wild-type ALK were immunoprecipitated with an anti-FLAG antibody and subjected to western blot analysis with anti-PY20. (**d**) *In vitro* kinase assay for wild-type ALK and its mutants using the synthetic YFF peptide as a substrate. (**e**) Western blot analysis of NIH3T3 cells stably expressing ALK mutants and wild-type ALK for their downstream effectors, STAT3 (pSTAT3), AKT (pAKT) and ERK (pERK). The total amount of each molecule is also shown together with an α-tubulin blot.

DNA was extracted from NB-1 cells and peripheral normal blood cells. For Southern blot analysis, 10 μg genomic DNA was restricted with *Eco*RI and loaded onto an agarose gel.[35] After electrophoresis, the DNA was transferred to polyvinylidene difluoride membranes and hybridized with radiolabeled probes for *ALK* exons 1–4 listed in Table 3. The signal intensity of each band was quantified and calculated using the ImageQuant 400 and ImageQuant TL software version 7 (GE Healthcare, Piscataway, NJ, USA).

Quantitative genomic PCR analysis

Quantitative genomic real-time PCR was performed using SYBR Green-based quantification (Bio-Rad Laboratories, Hercules, CA, USA). The standard curve method was used to calculate the target genome numbers in the NB-1 cell line. The relative target copy number was normalized to normal human genomic DNA as a calibrator. The primer sequences used for quantitative genomic PCR are shown in Table 3.

Transforming potential of ALK mutants

ALK^{WT}-FLAG and ALK^{F1174L}-FLAG were FLAG-tagged cDNAs for wild-type *ALK* and its F1174L mutant, respectively. FLAG-tagged cDNA for the

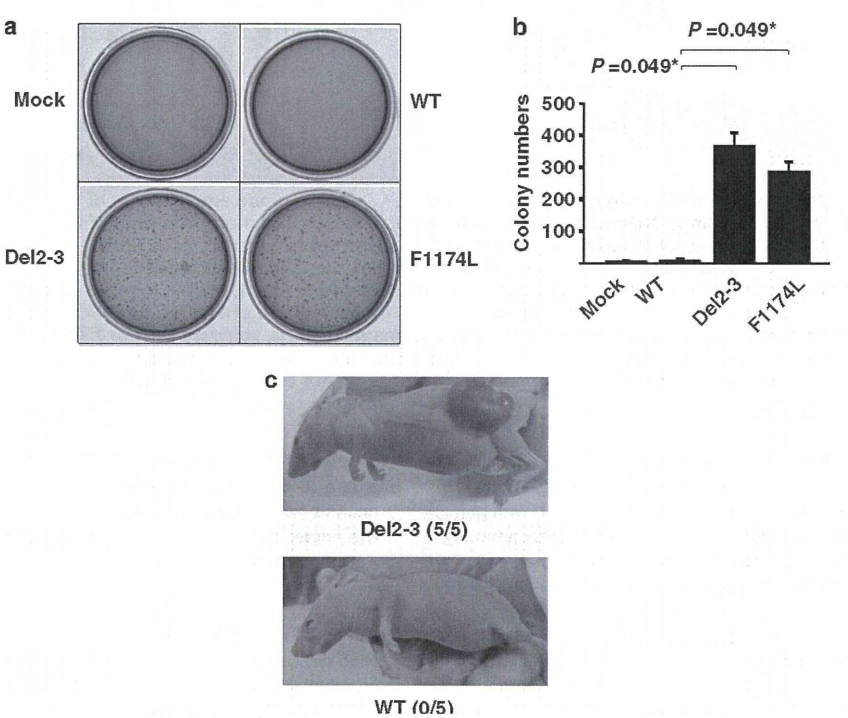

deletion mutant (*ALK*$^{del2\text{-}3}$-FLAG) was isolated from total RNA of NB-1 cells by high-fidelity PCR. After re-sequencing, each cDNA was constructed into the pcDNA3 expression plasmid and transfected into NIH3T3 cells using Effectene Transfection Reagents (Qiagen, Tokyo, Japan). Kinase assays were performed with stable clones in these constructs. For western blot analysis of mutant ALK and colony formation assays, NIH3T3 cells were stably transduced with wild-type and mutant ALK by retrovirus-mediated gene transfer. FLAG-tagged cDNA for wild-type and mutated ALK were then

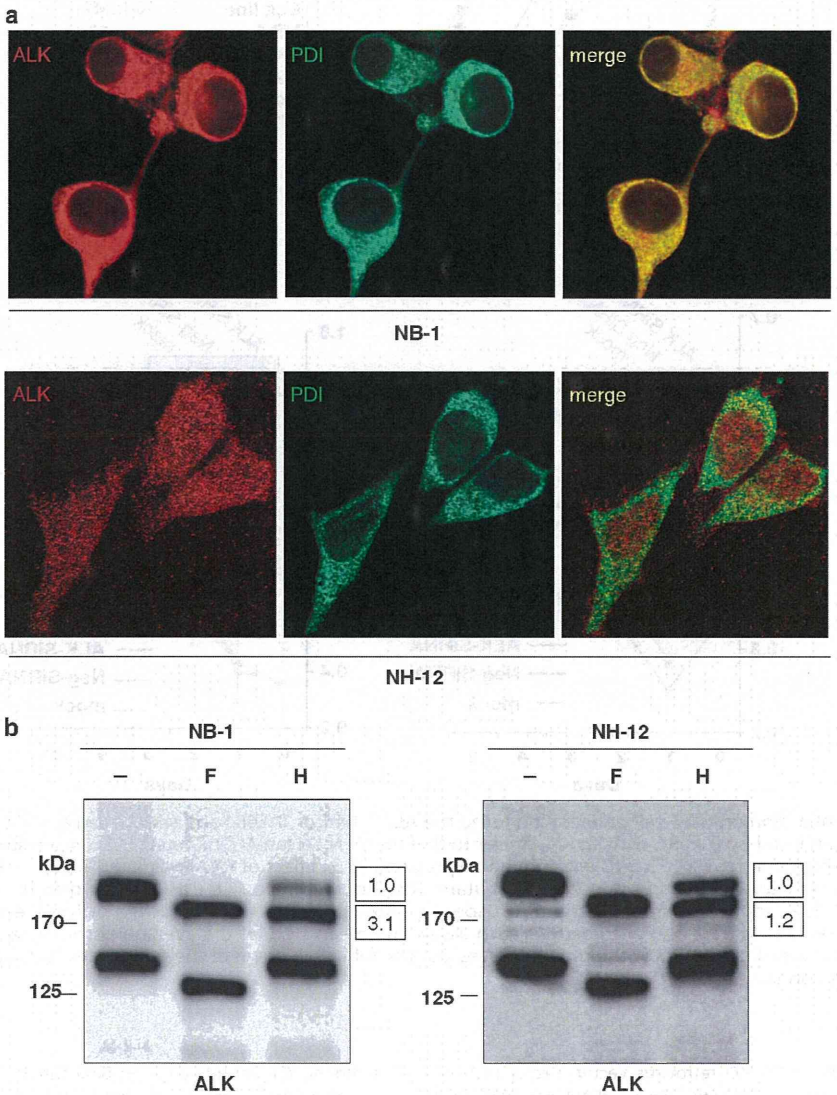

Figure 5. ER retention in the NB-1 neuroblastoma cell line and glycoprotein maturation. (**a**) Immunofluorescence confocal microscopy analysis of ALK ER localization in the neuroblastoma cell lines. The NB-1 and NH12 neuroblastoma cell lines were immunostained with the indicated antibodies and imaged using immunofluorescence microscopy to demonstrate ALK and PDI (ER-specific marker) colocalization. Cells were immunostained for ALK (red) and PDI (green), respectively. (**b**) The band of ALK$^{del2\text{-}3}$ protein of NB-1 cells is endoglycosidase H sensitive. Cell lysates from the NB-1 and NH12 neuroblastoma cell lines were incubated with N-glycosidase F (lane 2, F) and endoglycosidase H (lane 3, H). Deglycosidation profiles were compared with untreated cell lysates (lane 1). Digestion products were analyzed by western blot analysis using monoclonal anti-ALK. Signal intensities of bands in the lane endoglycosidase H were quantified by densitometric scanning using the ImageQuant 400 and ImageQuant TL software version 7. Signal intensity of approximate190 kDa band that revealed sensitivity to endoglycosidase H in NB-1 cells showed 3.1-fold higher than that of upper band.

Figure 4. Oncogenic role of the aberrant truncated form of ALK. (**a**) NIH3T3 cells stably expressing mutant kinases (ALK$^{del2\text{-}3}$ and ALK^{F1174L}) showed increased colony formation in soft agar compared with cells expressing wild-type kinase. (**b**) The average numbers of colonies in triplicate experiments are plotted. Standard deviation is indicated. Results showing significant differences compared with experiments using wild-type ALK are indicated by asterisks with *P*-values. (**c**) *In vivo* tumorigenicity assay in nude mice. Tumor formation assay in nude mice in which 1.0×10^7 NIH3T3 cells expressed wild-type ALK and the ALK$^{del2\text{-}3}$ mutant by the calcium phosphate method. Tumor formation was evaluated 21 days after inoculation.

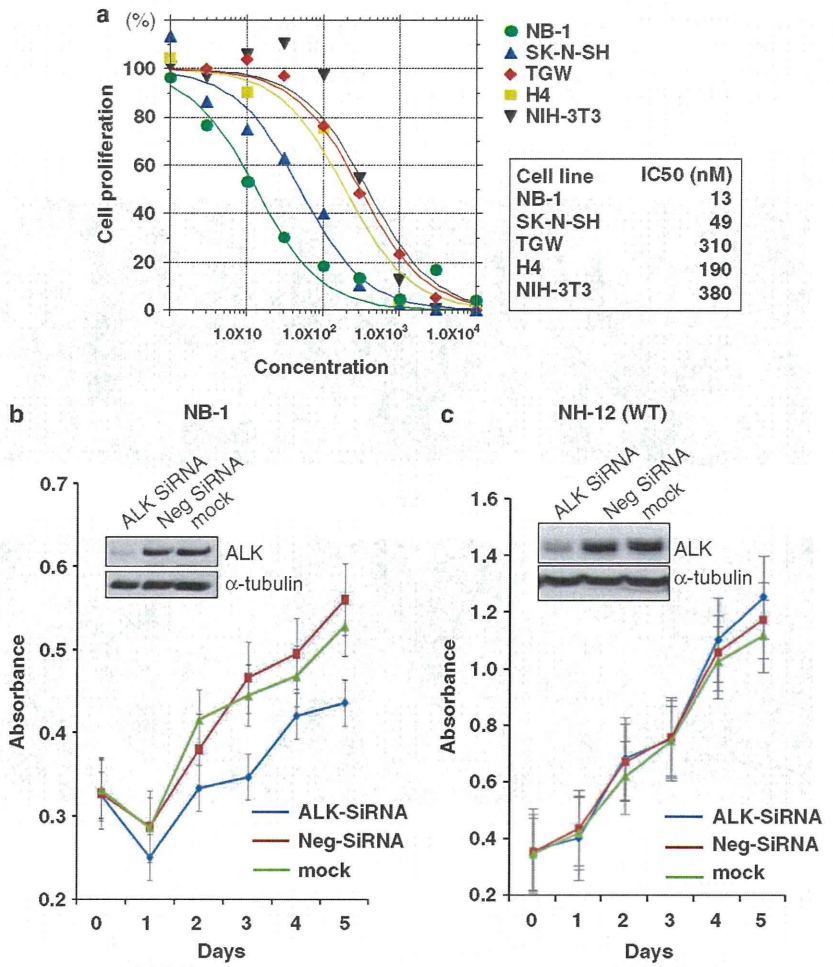

Figure 6. Effect of ALK inhibition on NB-1 cell proliferation using the ALK inhibitor TAE684 and siRNA-mediated ALK knockdown. (**a**) NB-1 cell growth was effectively inhibited by TAE684, with an IC_{50} similar to that for SK-N-SH (an *ALK*-mutated TAE684-sensitive neuroblastoma cell line), but substantially lower than that for NIH3T3 cells with no ALK expression. (**b**, **c**) Effect of RNAi-mediated ALK knockdown on cell proliferation in neuroblastoma cell lines expressing either the $ALK^{del2\text{-}3}$ mutant (NB-1) or wild-type ALK (NH-12). Cell growth was measured using the Cell Counting kit-8 after knockdown experiments using ALK-specific siRNAs, negative control siRNAs or mock experiments, in which absorbance was measured in triplicate and averaged for each assay. The mean ± s.d. of the average absorbance in three independent knockdown experiments was plotted to draw the growth curves. Successful knock down of the ALK protein was confirmed by anti-ALK blots using α-tubulin blots as controls.

constructed in the pGCDNsamIRESKO retrovirus vector. Vector plasmids were co-transfected with vesicular stomatitis virus-G cDNA into 293GP cells to obtain a retrovirus-containing supernatant, which was then transduced into 293GPG cells to stable cell lines capable of producing vesicular stomatitis virus-G-pseudotyped retroviral particles on induction.

Functional analyses of a short-form ALK

To evaluate the phosphorylation status of the ALK mutants, stable clone cell lysates were subjected to western blot analysis with anti-ALK and the antibody-specific pTyr1604 (Cell Signaling Technology, Danvers, MA, USA) of ALK. Immunoprecipitation with antibodies to FLAG (Sigma, St Louis, MO, USA) were subjected to western blot analysis with a generic antiphosphotyrosine antibody (PY20). Western blot analyses were also performed using anti-ERK1/2, anti-phospho-ERK1/2, anti-AKT, anti-phospho-AKT, anti-STAT3 and anti-phospho-STAT3 antibodies (Cell Signaling Technology). AKT and STAT3 phosphorylation signals were quantitated by densitometric scanning using the ImageQuant 400 and ImageQuant TL software version 7 (GE Healthcare). The *in vitro* kinase assay was performed with the synthetic YFF peptide (Operon Biotechnologies, Reutlingen, Germany), as described previously,[36] using stable clones in pcDNA vector constructs. We also used the *in vitro* kinase assay for wild-type and mutant *ALK* expression in NIH3T3 cells by retrovirus-mediated gene transfer using the poly-GluTyr peptide. Cell extracts were immunoprecipitated with anti-Flag antibody, and the expression was subjected to immunoblotting using anti-ALK antibody. ALK mutant kinase activity was measured using a non-radioactive isotope solid-phase enzyme-linked immunosorbent assay in the Universal Tyrosine Kinase Assay kit (Takara Bio, Osaka, Japan). Assays were performed in 40 mM Tris (pH 7.4), 20 mM $MgCl_2$, 2 mM dithiothreitol and 0.1 mg/ml bovine serum albumin buffer.

Transforming potential of short-form ALK

For colony assays, 1×10^3 stably transfected NIH3T3 cells were mixed in 0.4% agarose with 10% fetal bovine serum-Dulbecco's modified Eagle's medium and plated on 0.6% agarose-coated 35-mm dishes. After culturing for 14 days, colonies measuring 0.1 mm in diameter were counted. Colonies were quantified during triplicate experiments. Tumor formation

Table 3. Primer sets used in this study

	Primer sequence (5′→3′)		*Annealing temperature (°C)*
	Forward	*Reverse*	
RT-PCR analyses			
ALK exon 1/5	CTTCTCTTCCAGATCTTCGG	ATTCAGGGCAAAGAAGTCCAC	55
Exon 1/2	AAGCAGTTGGTGCTGGAGCT	TTTGACTTCCCCTGTGAGCT	55
Exon 2/4	CATAGCTCCTTGGAATCACC	ATGAGGAGCAGCAGTGAGCA	55
Exon 4/5-6	TTCTCAACACCTCAGCTGAC	ACTGCAGTGAAGGAACATCC	55
Exon 5/8-9	GAAACCGCAGCTTGTCTGCA	CGATCAAGAGCTCTCCATGT	55
Exon 8/12	AAGTGCTACAGTGACCAGTG	TAGCGGAGAGGACAAGATC	55
Exon 11/14	ATATCTCCATCAGCCTGGAC	AAGAACACCATGATGCGGTC	55
Exon 13/15-16	CCTGAAAGGCATCCAGATCT	AAGATGAAGGATGGAGTGCC	55
Exon 15/17	AATCCGTGTGAACAGAAGCG	TGGAGGAGGCGGAGGATATA	55
Exon 17/19-20	AAATCTTTGCAGGAGGGTGC	GCGTCTCCTGCATTGTGTCA	55
Exon 20/23	TTTCTCCGGCATCATGATTG	CTCATGGAAGCCCTGATCAT	55
Exon 23/26	TGCCTGAAGTGTGCTCTGAA	GATTGGAGACTTCGGGATGG	55
Exon 26/30	AGAAACTGCCTCTTGACCTG	GGACCCGGATGTAATCAACA	55
Exon 29/30	GGAGAGGATTGAATACTGCA	GTTGCACAAGGTCCACGGAT	55
Exon 30/30	TGCAGAGATCTCTGTTCGAG	GTTGCACAAGGTCCACGGAT	55
Exon 30/30	TAACGTTGCAACTGGGAGAC	GTTGCACAAGGTCCACGGAT	55
β-Actin	CTTCTACAATGAGCTGCGTG	TCATGAGGTAGTCAGTCAGC	55
Southern blot analyses			
ALK exon 1	AGAGTCTGGCAGTTGACTTC	TGCTCACAAACAGTCCCGAAG	60
Exon 2	TCAACTCAGTCTACTGGTGG	GGATATGGCAGACACAAAGC	60
Exon 3	AGCCCTGTGGTATTGACAAC	AGATGGGACTTGTCTTCCTC	60
Exon 4	AGAATGGAGGAAGAAGGCTG	GTAATTGCTCAACCTGGACC	60
TUBA4A	CTCTCACACTCTGGTATCTC	CTGACCATTAGCACAGTCTC	60
Quantitative genomic PCR analyses			
ALK exon 1	CTCAGCGAGCTGTTCAGTTG	CAGTCCCGAAGATCTGGAAG	55
Intron 1	CTGCTTGGTTCCTCACATCC	GTCTGAGTCATTGGCTAATCTCA	55
Exon 2	ACCCAAGCACATGGATCAG	GATGAGACAGGAAAGGGAAGG	55
Intron 2	GGTATACACGTGCCATGGTG	CCAAATACGGCATGTTCTCA	55
Exon 3	GGAGTGCAGCTTTGACTTCC	CTGGGCATCTCCTTAGAACG	55
Intron 3	TGGCATGATTGATTACCCAAG	CTGGAGATCACCCTTTGAGG	55
Exon 4	CAACACCTCAGCTGACTCCA	CTCTCTTGCAGCCTCGTTG	55

Abbreviations: ALK, anaplastic lymphoma kinase; RT-PCR, reverse transcription-polymerase chain reaction.

assay was performed in nude mice, in which 1.0×10^7 NIH3T3 cells expressing wild-type *ALK* and $ALK^{del2\text{-}3}$ mutant were injected by the calcium phosphate method. Tumor formation was evaluated 21 days after inoculation as described previously.[6]

Immunofluorescence

Cells were fixed for 10 min with 4% paraformaldehyde and washed three times with phosphate-buffered saline. After 1 h of blocking in phosphate-buffered saline containing 4% donkey serum and 0.1% Triton X-100/phosphate-buffered saline, the cells were incubated for 2 h in the same buffer with polyclonal anti-ALK (Santa Cruz Biotechnology, Santa Cruz, CA, USA) and monoclonal anti-PDI (Abcam, Cambridge, MA, USA), respectively. The cells were then washed three times with phosphate-buffered saline before and after incubation with anti-mouse IgG Alexa Fluor 488 and anti-rabbit IgG Alexa Fluor 594-conjugated secondary antibodies, respectively, (Invitrogen, Carlsbad, CA, USA). The cells were then mounted in Prolong Gold (Invitrogen). Confocal laser microscopy was performed using a Fluoview 10 000 confocal microscope (Olympus, Tokyo, Japan). Colocalization of ALK and PDI was quantified using the Pearson's correlation coefficient and determined through correlation analysis with a Fluoview 1000 software.[37]

Deglycosylation of ALK with N-glycosidase F, N-glycosidase H and O-glycosidase

Proteins from cell lysates obtained from neuroblastoma cell lines NB-1 and NH-12 were incubated with N-glycosidase F and endoglycosidase H for deglycosylation (New England Biolabs, Ipswich, MA, USA), following the manufacturer's instructions.[18] The samples were then used for immunoblotting with anti-ALK antibody. Signal intensities of bands in the lane endoglycosidase H were quantified by densitometric scanning using the ImageQuant 400 and ImageQuant TL software version 7.

ALK inhibition by an ALK inhibitor and siRNA-mediated knockdown in neuroblastoma cells

A partial *ALK*-deleted neuroblastoma-derived cell line (NB-1), *ALK*-mutated neuroblastoma-derived cell lines (SK-N-SH and TGW) and a glioblastoma-derived cell line (H4) were cultured with varying concentrations of the ALK inhibitor TAE684,[8] and cell growth was measured using the CellTiter-Glo Luminescent Cell Viability Assay (Promega, Tokyo, Japan). NIH3T3 cells were used as a control. The IC_{50} value of TAE684 against NB-1 cells was calculated by nonlinear regression (variable slope) using the GraphPad Prism 5 software (GraphPad, La Jolla, CA, USA). NB-1 and NH-12 cells with wild-type ALK were transfected with either an *ALK*-specific siRNA or a nonspecific siRNA, as described previously.[7] To assess the effect of ALK knockdown on cell growth, cells were seeded in 96-well plates at a concentration of 1.0×10^4 cells per well 24 h before transfection and assayed using the Cell Counting kit-8 (Dojindo, Kumamoto, Japan). We also performed an siRNA-mediated ALK knockdown cell proliferation assay using a cell counter and 6-well plates. These cells were seeded in 6-well plates at a concentration of 2.0×10^5 cells per well 24 h before transfection. The number of cells was counted after 72 h using cytorecon (ECI, Tokyo, Japan).